THE JOURNAL OF BIOLOGICAL CHEMISTRY VOL. 285, NO. 20, pp. 15245–15255, May 14, 2010

Residues Contributing to the Na^+-binding Pocket of the *SLC24* Na^+/Ca^{2+}-K^+ Exchanger NCKX2*[S]

Received for publication, December 4, 2009, and in revised form, March 4, 2010 Published, JBC Papers in Press, March 15, 2010, DOI 10.1074/jbc.M109.090738

Haider F. Altimimi[1], **Eric H. Fung**[2], **Robert J. Winkfein, and Paul P. M. Schnetkamp**[3]

From the Department of Physiology & Pharmacology, Hotchkiss Brain Institute, University of Calgary, Calgary, Alberta T2N 4N1, Canada

Na^+/Ca^{2+}-K^+ exchangers (NCKX; gene family *SLC24*) are plasma membrane Ca^{2+} transporters that mediate the extrusion of one Ca^{2+} ion and one K^+ ion in exchange for four Na^+ ions. NCKX is modeled to have two sets of five transmembrane segments separated by a large cytosolic loop; within each set of transmembrane segments are regions of internal symmetry termed α_1 and α_2 repeats. The central residues that are important for Ca^{2+} and K^+ liganding and transport have been identified in NCKX2, and they comprise three central acidic residues, Glu^{188} in α_1 and Asp^{548} and Asp^{575} in α_2, as well as Ser/Thr residues one-helical turn away from these residues. In this study, we have scanned through more than 100 single-residue substitutions of NCKX2 for shifts in Na^+ affinity using a fluorescence assay to monitor changes in free Ca^{2+} in HEK293 cells treated with gramicidin to control intracellular Na^+. We have identified 31 residues that, when substituted, result in shifts in Na^+ affinity, either toward higher or lower K_m values when compared with wild type NCKX2 (K_m for Na^+ 58 mM). These residues include the central acidic residues Glu^{188}, Asp^{548}, and Asp^{575}, and their neighboring residues in α_1 and α_2, in addition to a number of newly investigated residues in transmembrane segment 3. Our results relate the identification of residues important for Na^+ transport in this study to those previously identified as important in the counter-transport of Ca^{2+} and K^+, lending support to the alternating access model of transmembrane transport.

Na^+/Ca^{2+}-K^+ exchangers (NCKXs; gene family *SLC24*)[4] are Ca^{2+} transport proteins, which are thought to physiologically operate as cellular Ca^{2+} efflux mechanisms by extruding one Ca^{2+} ion and one K^+ ion in exchange for four Na^+ ions (1); NCKX can also import Ca^{2+} into the cell upon reversal of the transmembrane Na^+ gradient (1) or carry out Ca^{2+} + K^+:Ca^{2+} + K^+ or Na^+:Na^+ self-exchange (2). NCKX proteins are preferentially distributed in the plasma membrane of excitable tissues. NCKX1 extrudes Ca^{2+} entering outer segments of retinal rod photoreceptors through cyclic nucleotide gated channels (1, 3). NCKX2 plays a similar role to NCKX1 in retinal cone outer segments (4, 5) and is widely distributed throughout brain neurons (6); NCKX2 knock-out leads to changes in synaptic plasticity at hippocampal Schaffer/CA1 synapses associated with deficits in tests of motor learning and spatial working memory (7) and sensitizes the brain to ischemic damage following middle cerebral artery occlusion (8). NCKX3 and NCKX4 have more widespread tissue distribution other than in brain, notably in smooth muscle tissues of aorta, intestine, and lung, as well as in thymus (9–11). NCKX5, on the other hand, is restricted to intracellular membranes of melanocytes and plays a critical role in skin and ocular pigmentation (12–14).

Our current topological model for NCKX2, as a prototypical member of the NCKX family, predicts two sets of five α-helical transmembrane segments (TMs) separated by a large cytoplasmic loop (15) (see Fig. 8). NCKX2 shares with other Na^+-coupled membrane transporters the feature of a set of internal repeats in hydrophobic domains whose sequence is inverted with respect to the plane of the membrane (15–21); in Na^+/Ca^{2+} exchangers those repeats are termed α_1 and α_2, which in NCKX2 comprise TMs 2 and 3 and TMs 8 and 9, respectively, and are the regions of highest sequence identity in all five members of the NCKX family (Fig. 1; see also Fig. 8). We have shown previously that the α repeats of NCKX2 are important for its transport function and are packed closely within the plane of the plasma membrane (22, 23). Two central acidic residues, Glu^{188} in α_1, and Asp^{548} in α_2, were crucial in governing the affinity of NCKX2 for transported Ca^{2+} as well as K^+; charge-conservative substitution of either residue caused 100- and 10-fold decreases in the apparent affinities for Ca^{2+} and K^+, respectively, whereas size-conservative substitutions completely abolished cation transport (24). In addition, we found Asp^{575} in TM9 to be a unique residue that defines K^+ dependence in NCKX, because substitution with either Asn or Cys rendered NCKX2 K^+-independent (25).

The alternating access model for plasma membrane cotransporters or exchangers predicts that the same binding pocket of the transporter would bind counter-transported substrates when the transporter is in the cytoplasmic configuration or in the extracellular facing configuration (26, 27). This suggests that the same residues may be important for both Na^+ and

* This work was supported in part by Grant MOP 81327 from the Canadian Institutes of Health Research (to P. P. M. S.).

[S] The on-line version of this article (available at http://www.jbc.org) contains supplemental Table S1 and Figs. S1–S5.

[1] Supported by Foundation Fighting Blindness-Canada and by Natural Sciences and Engineering Research Council of Canada graduate studentships.

[2] Recipient of a summer studentship from the Alberta Heritage Foundation for Medical Research.

[3] To whom correspondence should be addressed: 3330 Hospital Dr. NW, Calgary, AB T2N 4N1, Canada. Tel.: 403-220-6862; Fax: 403-210-7446; E-mail: pschnetk@ucalgary.ca.

[4] The abbreviations used are: NCKX, Na^+/Ca^{2+}-K^+ exchanger; TM, transmembrane segment; NCX, Na^+/Ca^{2+} exchanger; HEK293, human embryonic kidney 293 cells; wt, wild type; FCCP, carbonyl cyanide *p*-trifluoromethoxyphenylhydrazone.

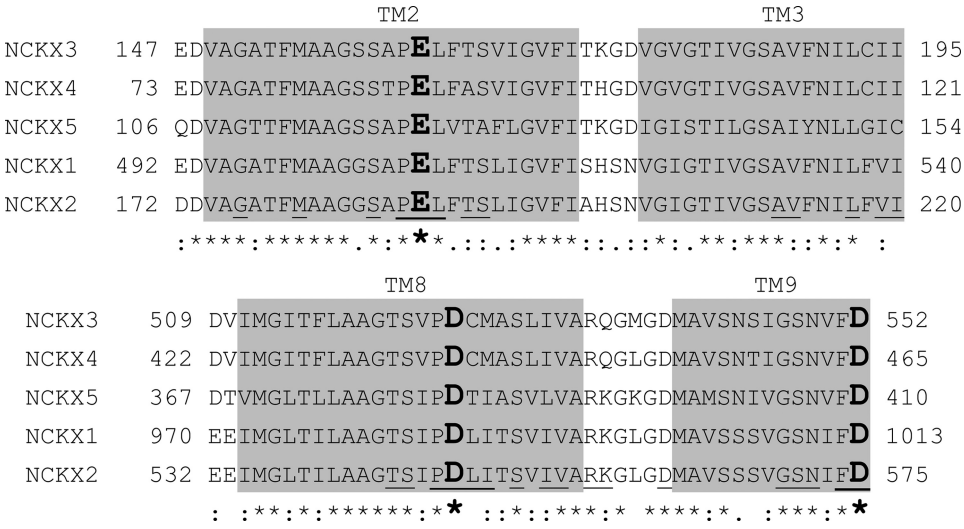

FIGURE 1. **Amino acid sequence alignment of human NCKX1–5 (NP_004718.1, NP_065077.1, NP_065740.2, NP_705932.1, and NP_995322.1) is shown in the sections through the α_1 (transmembrane segments 2 and 3) and α_2 (transmembrane segments 8 and 9) repeats, for which all residues were substituted and analyzed for shifts in Na_i^+ affinity in this study.** *Gray shading* demarcates modeled transmembrane α-helical segments (15). Positions critical for Ca^{2+} and K^+ transport, acidic residues Glu^{188}, Asp^{548}, and Asp^{575}, are highlighted by *large bold typeface* (24, 25). Residues analyzed in greater detail (as presented in Figs. 6 and 7) are *underlined*. Sequence alignment was performed using ClustalW2 (41). An *asterisk* denotes a strictly conserved residue in all of the sequences in the alignment, a *colon* denotes conserved substitutions observed, and a *period* denotes semi-conserved substitutions observed.

Ca^{2+}/K^+ transport and underscores the importance of examining the residues critical for Na^+ counter-transport in Na^+/Ca^{2+} exchangers. NCKX is especially interesting in this regard because it is characterized, alongside NCX, by the capacity to transport multiple Na^+ ions/cycle; moreover, both NCKX and NCX are unique in their absolute selectivity for Na^+ over any other alkali cation (28–30). To date, however, the residues involved in Na^+ transport in NCKX are unknown, except for our previous identification of Asp^{548} as a residue whose charge-conservative substitution dramatically increased Na_i^+ affinity; alongside Asp^{548}, we also identified substitution of Asn^{572} with Cys to affect Na_i^+ affinity (31). Herein, we extend our mutational analysis to 88 single-residue substitutions covering the α repeats and all 14 additional acidic residues of NCKX2 found in the two sets of five TMs. We report 31 residues whose substitution alters apparent Na_i^+ affinity and relate our current results to our previous findings of residues that are involved in the transport of Ca^{2+} and K^+ (24, 25).

EXPERIMENTAL PROCEDURES

All chemicals were purchased from Sigma-Aldrich unless otherwise specified. The fluo-based assay of NCKX Ca^{2+} influx activity in transiently transfected HEK293 cells and the use of gramicidin to measure Na^+ affinity have been described previously in Refs. 24 and 31, and only modifications are included herein. Briefly, HEK293 cells were transiently transfected with wild type, Myc-tagged, human short splice variant of NCKX2 (wt NCKX2) in pcDNA3.1 vector (Invitrogen) using calcium phosphate precipitation; single-residue substitutions were produced in this background (23). Two days following transfection, the cells had grown to confluency in 10-cm culture dishes, and the total population of cells from two culture dishes, transfected with the same construct, were trypsinized and resuspended in 300–500 μl of LiCl-EDTA buffer (150 mM LiCl, 20 mM HEPES, 6 mM D-glucose, 0.5 mM dithiothreitol, 0.25 mM sulfinpyrazone, 0.1 mM EDTA, pH adjusted to 7.4 with L-Arg). The suspension of cells transfected with the same construct was then split into two aliquots to be loaded separately with 2 μM fluo-4AM and 2 μM fluo-4FFAM (Molecular Probes) in 0.5% (v/v) final dimethylformamide concentration (cells were loaded with fluo-3AM in the case of Fig. 2 and supplemental Fig. S1). After 1 h, the cells were pelleted, washed with Li-EDTA buffer, and resuspended in 100–150 μl of Li-EDTA buffer for an additional hour before commencing functional measurements. For each experimental measurement, a 10-μl aliquot containing $\sim 2.5 \times 10^5$ cells was added to a cuvette containing 1990 μl of KCl-EDTA buffer (same composition as Li-EDTA buffer, but with KCl iso-osmotically replacing LiCl) placed in the thermostatted (25 °C) cuvette holder of an SLM Series 2 luminometer (SLM Instruments, Urbana, IL) with constant stirring via magnetic stirrer, and fluorescence was continuously recorded (excitation, 480 nm; bandwidth, 8 nm,; emission, 530 nm; bandwidth, 8 nm) integrated over 200-ms time bins (1-s time bins in the case of data in Fig. 2 and supplemental Fig. S1). The cells were treated in the cuvette with the ionophores gramicidin and FCCP (2 μM each, in 0.2% (v/v) final ethanol concentration); in the case of the data in Fig. 2 and supplemental Fig. S1, the cells were treated with 2 μM gramicidin and 0.4 μM thapsigargin (except where indicated). Four minutes following the addition of ionophores, 350 μM $CaCl_2$ was added to achieve 250 μM free $[Ca^{2+}]_o$; to initiate Ca^{2+} influx through NCKX2, NaCl was added (from 5 M stock) 10 s following $CaCl_2$ addition. At the end of each measurement, saponin (0.02% (w/v) final concentration) was added to release fluo-4 or fluo-4FF, and fluorescence was saturated by the addition of 10 mM $CaCl_2$.

Mutant NCKX2 protein expression levels were measured by Western blotting using a monoclonal anti-MYC antibody, and all of the mutants used in this study showed normal expression levels, although as described previously (24), mutant NCKX2 protein expression levels were slightly more variable when compared with our earlier studies using insect cell lines (23). A selected example of mutant NCKX2 expression levels is illustrated in supplemental Fig. S2. In this and our other studies using HEK293 cells, the emphasis is not to determine changes in V_{max} but changes in K_m values for Na^+, Ca^{2+}, and K^+. Nevertheless, we observed a good correlation between changes in V_{max} observed in HEK293 cells when compared with changes

observed in the insect cell system where protein expression and plasma membrane trafficking were carefully measured (23).

For each experimental measurement, fluorescence was normalized to F_{max} attained at the end of the measurement with addition of saponin. Rates of Ca^{2+} influx were computed from the initial period of linear fluorescence increase upon the addition of NaCl (initial linear Δ normalized fluorescence). The period of initial linear increase in fluorescence used for computing rates of Ca^{2+} influx varied in duration depending on the concentration of NaCl applied, but for wt NCKX2 was typically less than 5 s for the highest NaCl concentrations applied and was as long as 10 s for lower NaCl concentrations (10–20 mM). To integrate fluo-4 and fluo-4FF measurements carried out on the same cell suspension into a single normalized rate measure, we chose an initial rate value from a $[Na^+]$ that was measured with both fluo-4 and fluo-4FF and that produced a fluorescence signal within the dynamic range for both indicators and used this rate value to normalize all other initial linear Δ normalized fluorescence values for that given experiment. The rates measured in the absence of NaCl addition were used as zero base lines. SigmaPlot 11.0 was used to plot data and for regression of normalized rate values with the three-parameter Hill function $V = V_{max}[Na^+]^n/(K_m^n + [Na^+]^n)$.

For comparison across experiments from different transfections, initial linear rates from a given experiment were normalized with respect to their respective V_{max} value predicted from Hill function regression, except where indicated for single-residue substitutions that produced marked decreased affinities for $[Na^+]_i$ that were no longer fit with Hill functions with confidence (we chose 200 mM Na^+ as the upper limit for testing). In those cases we used the average of the normalized rate values measured at 175 and 200 mM Na^+ for normalization (150 and 200 mM Na^+ in the case of wt NCKX2). The experimental data are presented as the means ± S.D. and Hill function regression parameters ± standard error of the model. Statistical comparison of the effects of single-residue substitutions on K_m values was carried out by using the nonlinear dynamic fit regression function in SigmaPlot 11.0 on pooled data from at least three different transfections/experimental measurements and compared using *t* test as described in Ref. 32. To compare substitution mutants with marked decreased Na_i^+ affinity to wt NCKX2, we compared with two-tailed *t* tests the normalized rates averaged for 75 and 100 mM $[Na^+]_i$.

RESULTS

Initial Screen of Single-residue Substitutions of NCKX2 for Shifts in Na_i^+ Affinity—Previously, we used a fluo-3-based assay to measure the affinity of wt NCKX2 and the affinity of a number of single-residue substitution constructs for $[Ca^{2+}]_o$ and $[K^+]_o$ (24, 25). This assay was subsequently modified by using gramicidin to control internal $[Na^+]$ to obtain a measure of the affinity of wt NCKX2 for $[Na^+]_i$ (31). We initially used fluo-3 measurements of changes in $[Ca^{2+}]_i$ induced by the addition of a limited set of $[Na^+]$ in the presence of gramicidin to scan through 102 single-residue substitutions comprising the α_1 and α_2 regions, as well as all other acidic residues present in the two sets of five TMs and their short connecting loops (Fig. 2 and supplemental Fig. S1); except for residues ^{213}VFNILFVI^{220} (Fig. 1), these residue substitution mutants were previously analyzed for maximal activity with respect to wt NCKX2 (23). Nearly all residue substitutions resulted in mutant NCKX2 proteins whose functional activity we were able to resolve with the following exceptions: G176C, E188Q, G210A/C/V, S211A/C/T, N215A/D/Q, A542S, T544C, D548N, K558N, and D575E showed insufficient (<1%) or no functional activity (see supplemental Fig. S1 for selected examples), although protein expression was very similar for all of the substitutions examined (*e.g.* supplemental Fig. S2 shows that the nonfunctional Asn^{215} substitutions showed normal protein expression). This assay proved efficient, and the results were highly reproducible, giving us a broad representation of the range of phenotypes for altered $[Na^+]_i$ affinity attained by various single-residue substitutions (Fig. 2). Several single-residue substitutions resulted in marked shifts in the affinity of NCKX2 for Na_i^+ affinity. *Panels C* and *D* of Fig. 2 show selected substitutions that appeared to have increased and decreased Na_i^+ affinity, respectively. However, most of the 102 single-residue substitutions tested did not appear to have altered $[Na^+]_i$ affinity, despite reduced V_{max} for many single-residue substitutions (Fig. 2*B*). From the results of our initial screen, we selected 39 residues that appeared likely to have altered Na^+ affinity to test in greater detail, as well as some that appeared unaltered but with diminished functional activity to serve as controls, as described below. For most single-residue substitution mutants, we tested substitutions with Ala and in a few cases with Cys (Ala with Ser); for charged residues, we tested both charge- and size-conservative substitutions.

Combined Use of Fluo-4 and Fluo-4FF to Increase Dynamic Range of $[Ca^{2+}]_i$ Measurement—We proceeded with improved $[Na^+]_i$ affinity measurements that account for the other major cellular Ca^{2+} handling mechanism of HEK293 cells: mitochondria— hence the use of FCCP; the contributions of sarco/endoplasmic reticulum Ca^{2+}-ATPase and plasma membrane Ca^{2+}-ATPase are negligible under our experimental conditions (31). In all our experiments an external Ca^{2+} concentration of 250 μM was used to drive Ca^{2+} influx via reverse exchange; this Ca^{2+} concentration represents a compromise between minimizing competition between external Ca^{2+} and Na^+ on the one hand and minimizing Ca^{2+} influx via other pathways, *e.g.* store-operated Ca^{2+} channels, on the other hand (supplemental Fig. S3 and legend). In the absence of mitochondrial Ca^{2+} sequestration, wt NCKX2-mediated increases in free Ca_i^{2+} were large, which necessitated the use of the lower affinity Ca^{2+} indicator fluo-4FF. This assay was previously used to measure the $[Na^+]_i$ affinities of wt NCKX2 and two single-residue substitutions with increased $[Na^+]_i$ affinity: D548E and N572C (31). Because the Na^+ dependence of Na^+/Ca^{2+} exchangers is a sigmoidal function resultant of the cotransport of multiple Na^+ ions, a wide range of $[Na^+]$-mediated changes in free $[Ca^{2+}]_i$ must be tested, and hence we decided to make simultaneous use of the two Ca^{2+} indicators with the most useful dynamic response range for our measurements, fluo-4 for lower range $[Ca^+]_i$ changes (Molecular Probes reported K_d = 0.35 μM) and fluo-4FF for higher range $[Ca^+]_i$ changes (Molecular Probes reported K_d = 9.7 μM). We also tested fluo-5N (Molecular Probes reported K_d for Ca^{2+} = 90 μM) but did not find differences in the initial linear Δ normalized fluo-

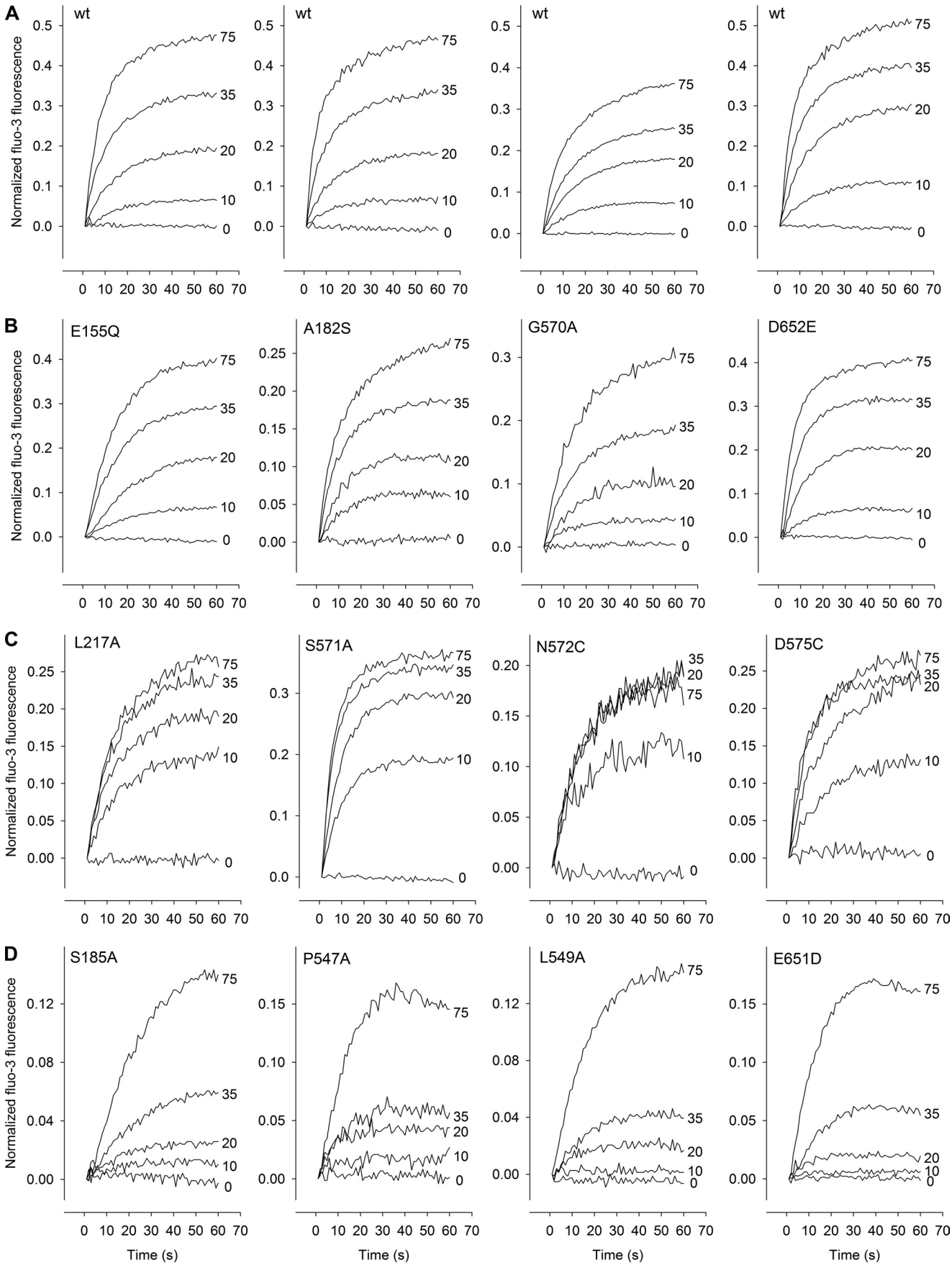
A
wt
wt
wt
wt
B
E155Q
A182S
G570A
D652E
C
L217A
S571A
N572C
D575C
D
S185A
P547A
L549A
E651D
Normalized fluo-3 fluorescence
Time (s)
75
35
20
10
0

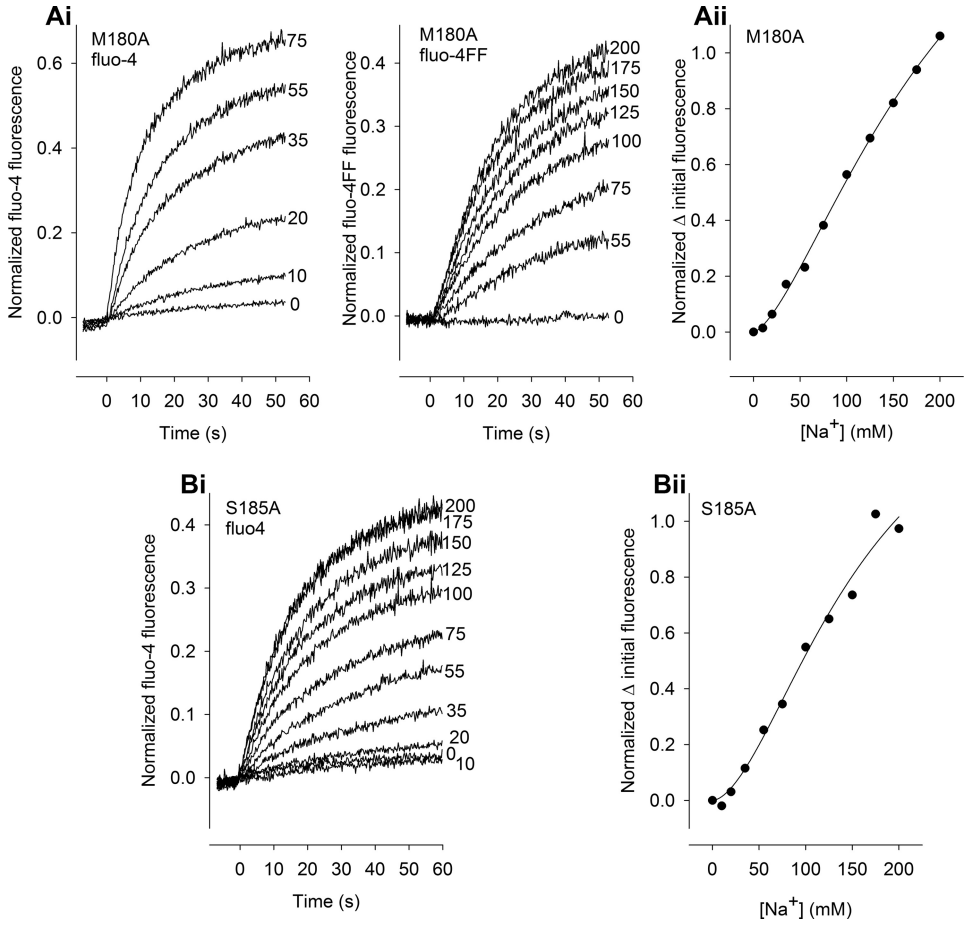

FIGURE 3. **Exemplar high resolution measurements of changes in $[Ca^{2+}]_i$ to derive a measure for Na_i^+ affinity of NCKX2 single-residue substitutions.** *A*, *panel i*, *left panel*, HEK293 cells expressing M180A loaded with fluo-4 were treated with 2 μM FCCP and 2 μM gramicidin, and the indicated Na^+ (mM) was added (at time 0) in the presence of 250 μM Ca^{2+} in buffered 150 mM KCl medium. *Right panel*, HEK293 cells expressing M180A from the same suspension as in the *left panel* were separately loaded with fluo-4FF, and the indicated $[Na^+]$ (mM) was added (at time 0) in the presence of 250 μM Ca^{2+} in buffered 150 mM KCl medium. *Panel ii*, rates were derived as described in detail under "Experimental Procedures." *B*, *panel i*, HEK293 cells expressing S185A loaded with fluo-4 were treated with 2 μM FCCP and 2 μM gramicidin, and the indicated $[Na^+]$ (mM) was added (at time 0) in the presence of 250 μM Ca^{2+} in buffered 150 mM KCl medium. *Panel ii*, rates were derived as described in detail under "Experimental Procedures." Exemplar traces are representative of two other experiments.

rescence when compared with fluo-4FF (supplemental Fig. S4). Fig. 3 shows exemplar measurements of two α_1 repeat substitution mutants: M180A and S185A, with decreased $[Na^+]_i$ affinity. Substitution of Met^{180} with Ala in NCKX2 reduced the V_{max} to 44% (see supplemental Table S1 for comparison against wt NCKX2 of V_{max} for all single-residue substitution mutants examined in detail in this study), but nevertheless, the $[Ca^{2+}]_i$ changes induced by the addition of $[Na^+]$ higher than 75 mM resulted in saturation of fluo-4 and were therefore additionally measured in parallel from the same suspension of cells loaded with fluo-4FF. The rates of initial linear change in $[Ca^{2+}]_i$ derived from the measurements shown in Fig. 3*A* indicated a substantially decreased affinity for $[Na^+]_i$ with respect to wt NCKX2; the Hill function regression predicted a K_m for $[Na^+]_i$ of M180A of 210 mM and a Hill coefficient of 1.5, whereas the affinity of wt NCKX2 for $[Na^+]_i$ was 58 ± 2 mM (Hill coefficient = 2.7 ± 0.3, n = 5; Fig. 4, *top left panel*; see also summary data in Fig. 6). S185A exhibited considerable reduction in V_{max} to 7% that of wt NCKX2, but by utilizing the higher affinity fluo-4, we were able to resolve small differences in the initial linear Δ normalized fluorescence (Fig. 3*B*). Rate derivation and Hill function regression of the exemplar measurement shown in Fig. 3*B* for S185A predicted a K_m for $[Na^+]_i$ of 161 mM (Hill coefficient 1.7). These results illustrate the high temporal resolution, as well as dynamic range of our measurements using fluorescence emission from a large ensemble of cells in cuvettes, where we were reliably able to resolve $[Ca^{2+}]_i$ transport of mutant constructs with activity as low as 1% of wt NCKX2.

Range of Shifts in $[Na^+]_i$ Produced by Substitutions within α_1 and α_2—Fig. 4 shows examples of the range of phenotypes observed for the subset of selected substitution mutants that were analyzed with fluo-4FF and/or fluo-4 in this study. Some substitutions resulted in only a moderate shift in Na_i^+ affinity, with respect to wt NCKX2 (Fig. 4, *top left panel*), and the resultant normalized rates were well fit with the Hill equation. The example of slight decreased Na_i^+ affinity shown in the *top right panel* of Fig. 4 is I554T; the K_m for $[Na^+]_i$ was 80 ± 3 mM (Hill coefficient = 2.4 ± 0.1, n = 3). This particular mutant was of interest to us because an Ile to Thr mutation was found in the equivalent position of the retinal rod NCKX1 gene of two unrelated retinal disease patients (33). Some substitution mutants produced strong shifts to higher Na_i^+ affinity, a phenotype we reported on previously for D548E and N572C (31). In all of these cases, the normalized rate values increased steeply in the range of $[Na^+]_i$ 10–75 mM and declined

FIGURE 2. **Initial screening through NCKX2 single-residue substitutions for shifts with respect to wild type NCKX2 in Na_i^+ affinity.** $[Ca^{2+}]_i$ was measured in response to the addition of the indicated Na^+ (in mM at time 0) in fluo-3 loaded HEK293 cells transfected with the indicated constructs and treated with 2 μM FCCP and 2 μM gramicidin in the presence of 250 μM Ca^{2+} in buffered 150 mM KCl medium (see "Experimental Procedures"). The fluorescence values were normalized with respect to the total of fluo-3 loaded in the cells by saponin permeabilization in the presence of saturating Ca^{2+}. Note that fluorescence measures here were integrated into 1.0-s time bins; in later experiments, fluorescence measures were integrated into 200-ms time bins. *A*, exemplar measurements for wild type NCKX2. *B*, exemplars of selected substitutions that appeared near wild type NCKX2 in Na_i^+ affinity. *C*, exemplars of selected substitutions that resulted in an apparent increase in Na_i^+ affinity. *D*, exemplars of selected substitutions that resulted in an apparent decrease in Na_i^+ affinity. The *traces* represented in this figure are representative of at least one other experiment.

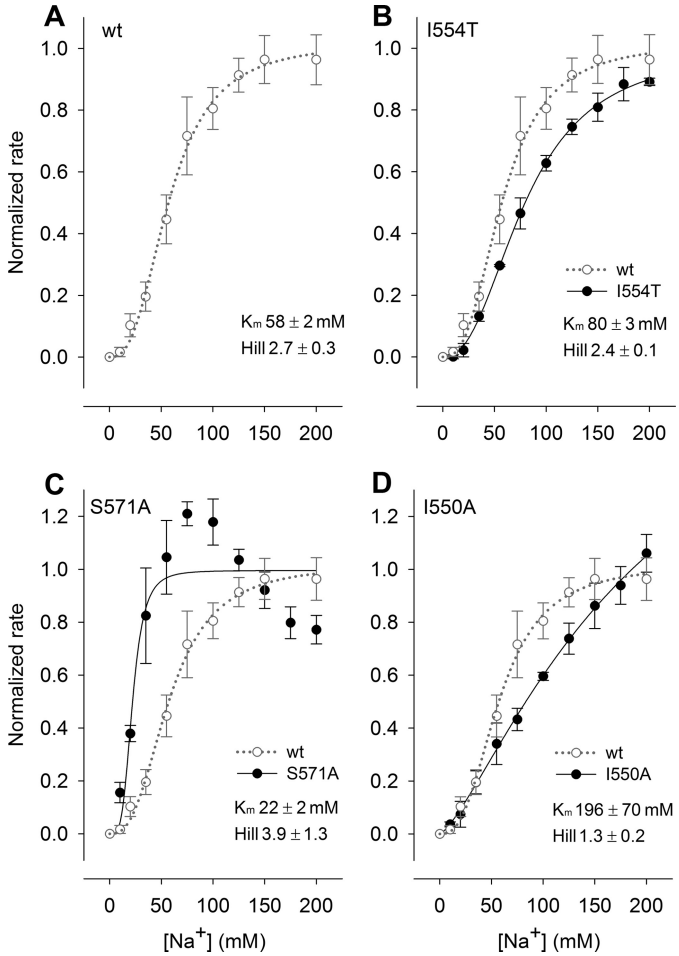

FIGURE 4. **Range of phenotypes in Na_i^+ affinity produced by single-residue substitutions in NCKX2.** *A*, average normalized rates for wild type NCKX2; the data points represent the means ± S.D. (n = 5), Hill function dynamic regression using SigmaPlot 11.0 predicted K_m for $[Na^+]$ of 58 ± 2 mM (standard error of the model), Hill coefficient 2.7 ± 0.3 (*dotted line*). *B*, example of single-residue substitution I554T (*solid black circles*) resulting in a slight decrease in $[Na^+]_i$ affinity; K_m for $[Na^+]$ = 80 ± 3 mM, Hill coefficient = 2.4 ± 0.1 (n = 3, *solid line*); wt NCKX2 is also shown for comparison (*open gray circles*, *dotted gray line*). *C*, example of single-residue substitution S571A (*solid circles*) resulting in an increase in $[Na^+]_i$ affinity; K_m for $[Na^+]$ = 22 ± 2 mM, Hill coefficient = 3.9 ± 1.3 (n = 3, *solid line*). *D*, example of single-residue substitution I550A (*solid circles*) resulting in a substantial decrease in $[Na^+]_i$ affinity; K_m for $[Na^+]$ = 196 ± 70 mM, Hill coefficient = 1.3 ± 0.2 (n = 3, *solid line*); Such substitutions that were not well fit with Hill functions were analyzed separately (see Fig. 7).

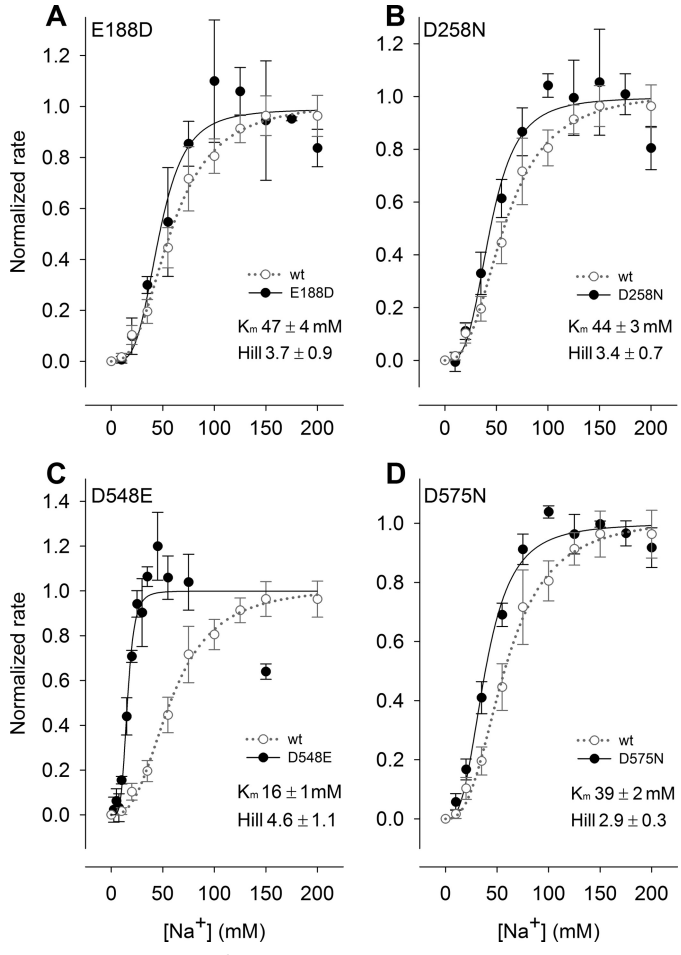

FIGURE 5. **Shifts in Na_i^+ affinity produced by substitutions of central acidic residues of NCKX2.** *A*, E188D (*solid circles*) K_m for $[Na^+]$ = 47 ± 4 mM, Hill coefficient = 3.7 ± 0.9 (n = 3, *solid line*); wt NCKX2 is also shown for comparison (*open circles*, *dotted line*). *B*, D258N (*solid circles*) K_m for $[Na^+]$ = 44 ± 3 mM, Hill coefficient = 3.4 ± 0.7 (n = 3, *solid line*). *C*, D548E (*solid circles*) K_m for $[Na^+]$ = 16 ± 1 mM Na^+, Hill coefficient = 4.6 ± 1.1 (n = 3, *solid line*); these data were adapted from our previously published study (31) and are analyzed using the same method employed in this study for all single-residue substitutions (see text for details). *D*, D575N (*solid circles*) K_m for $[Na^+]$ = 39 ± 2 mM, Hill coefficient = 2.9 ± 0.3 (n = 3, *solid line*).

for higher $[Na^+]_i$ tested; this correlated with increased Hill coefficient values (supplemental Table S1). In the example shown in the *bottom left panel* of Fig. 4, S571A, the normalized rates at the highest $[Na^+]_i$ tested declined by ~30% from the highest normalized rate value attained by the addition of 75–100 mM Na_i^+. The decline in normalized rates probably results from enhanced competition between Na^+ and Ca^{2+} at the exoplasmic configuration of NCKX mutants with large shifts to increased Na_i^+ affinity. The K_m for $[Na^+]_i$ derived from the Hill function regression for S571A was 22 ± 2 mM (Hill coefficient 3.9 ± 1.3, n = 3). In the fourth category of observed phenotypes, we found some substitution mutants displayed large decreases in $[Na^+]_i$ affinity, and the derived normalized rates did not appear to approach saturation at our upper limit for Na^+ addition of 200 mM and hence were poorly fit by the Hill equation; this is exemplified in the *bottom right panel* of Fig. 4 by I550A. The K_m for $[Na^+]_i$ was 196 ± mM 70 (Hill coefficient = 1.3 ± 0.2, n = 3). These single-residue substitution mutants typically had low Hill coefficient values (see supplemental Table S1). To analyze these residue substitutions, we normalized the rates observed at Na^+ concentrations of 75 and 100 mM to the average of the rate observed at the two highest Na^+ concentrations tested (*i.e.* 175 and 200 mM) and compared the results with the values obtained by this procedure for wt NCKX2. The results are shown in Fig. 7.

Mutations of Mid-membrane Plane Acidic Residues—There are only four strictly conserved mid-membrane plane acidic residues in our topological model of NCKX. Asp^{548} and Glu^{188} were crucial for Ca^{2+} and K^+ transport, whereas Asp^{258} was also important, but substitutions in that position produced shifts in Ca^{2+} and K^+ affinity to a lesser extent than either Asp^{548} or Glu^{188}. Asp^{575}, on the other hand, was found to be critical for defining K^+ dependence, because substitutions with either Asn or Cys rendered NCKX2 K^+-independent (24, 25).

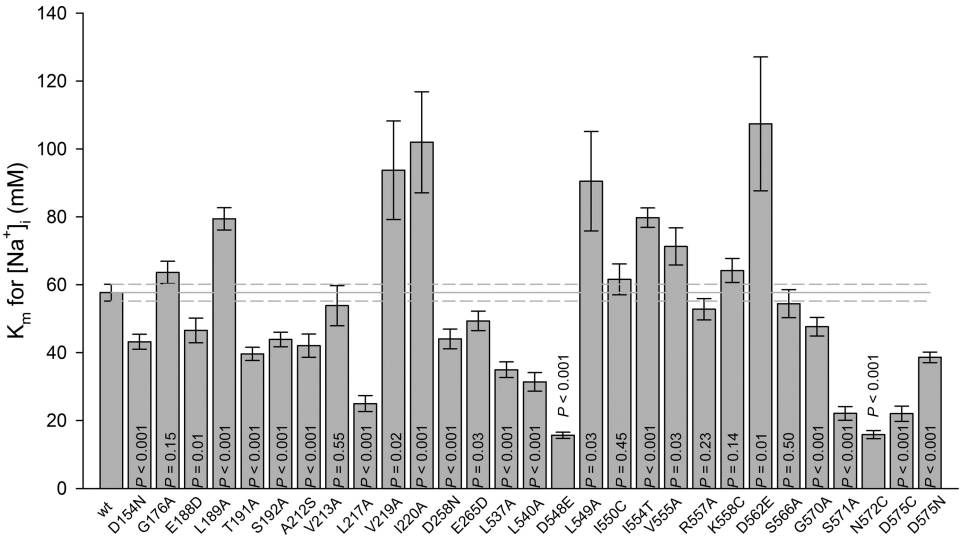

FIGURE 6. **Summary data of comparison of shifts in Na_i^+ affinity of single-residue substitutions with respect to wild type NCKX2.** The values represent the means ± S.E. of the model of K_m for Na_i^+ (mM) produced from Hill function regression analysis ($n = 3$ for all, except for wt, $n = 5$). Comparison against wt was carried out using two-tailed *t* test, with the indicated *p* values.

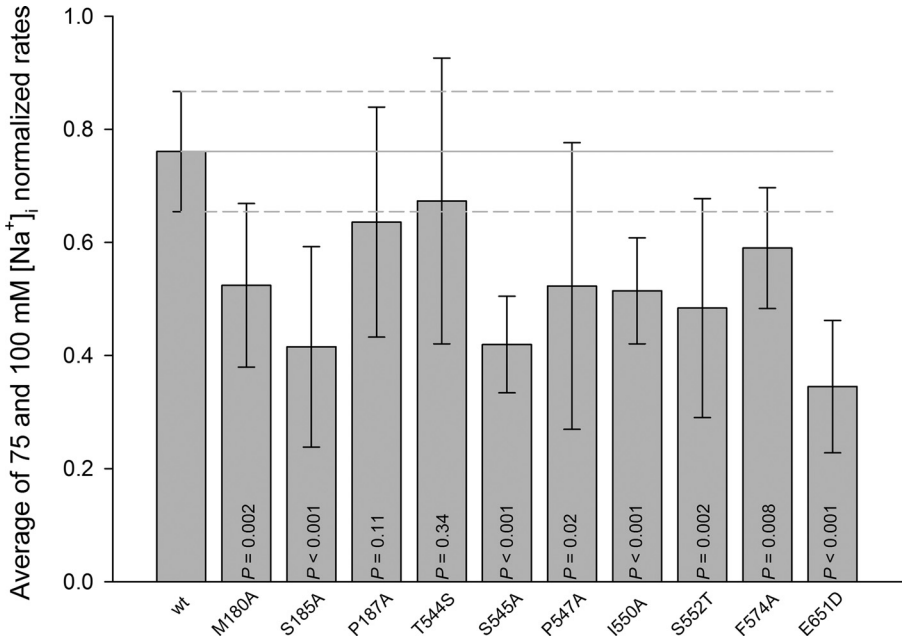

FIGURE 7. **Analysis of single-residue substitutions of NCKX2 that resulted in substantial decrease in apparent Na_i^+ affinity.** The normalized rates measured with the addition of 75 and 100 mM Na^+ were pooled, averaged, and then compared against wt NCKX2. The values represent the means ± S.D. ($n = 3$ for all, except for wt, $n = 5$ and P187A, $n = 4$). Comparison against wt was carried out using two-tailed *t* test, with the indicated *p* values.

We previously reported that D548E results in a substantial increase in Na^+ affinity, producing a shift to 16 ± 1 mM Na^+ (Hill coefficient 4.6 ± 1.1, $n = 3$; Figs. 5*C* and 6) (31). Its counterpart in α_1, E188D, on the other hand resulted in only a modest shift in Na_i^+ affinity, also to increased Na^+ affinity; K_m = 47 ± 4 mM, Hill coefficient = 3.7 ± 0.9 ($n = 3$; Figs. 5*A* and 6). Note that the V_{max} of E188D was substantially reduced to 3% that of wt NCKX2, whereas D548E V_{max} was reduced to 43% that of wt NCKX2. It is also worth noting that those substitutions tested (charge-conservative) were the only functional constructs; any other substitutions we tested for those positions resulted in a complete loss of functional activity. The substitution D258N, which is modeled to be in the mid-plane of TM4 (see Fig. 8), was also found to result in a modest but nonetheless significant increase in Na_i^+ affinity, K_m 44 ± 3 mM (Hill coefficient 3.4 ± 0.7, $n = 3$; Figs. 5 and 6). Substitution of Asp^{575} also resulted in a significant increase in Na^+ affinity; we tested the two substitution constructs produced in our lab that resulted in functional protein: D575C and D575N (we also produced D575E, but it showed no measurable activity (25)). The K_m of D575N was 39 ± 2 mM Na^+ (Hill coefficient = 2.9 ± 0.3, $n = 3$; Figs. 5*D* and 6), whereas the K_m for D575C was 22 ± 2 mM Na^+ (Hill coefficient = 4.3 ± 1.3, $n = 3$). Notice that with E188D, D258N, and D575N, there is a trend for the normalized rates at the highest $[Na^+]_i$ tested to decrease from the value of the true V_{max}, albeit not as pronounced as was the case for D548E and S571A shown in Figs. 5*C* and 4*C*, respectively. We found these trends to correlate with affinity for Na_i^+, and so the decrease in normalized rate at high $[Na^+]_i$ for D575C, which has a higher affinity for Na_i^+ than D575N (both had relatively similar levels of functional activity) was much more pronounced than D575N (supplemental Fig. S5).

Extracellular Facing or Cytoplasm Facing Charged Residues—We selected several charged residues that are located at the membrane interface in our topological model: D154N, R557A, K558C, D562E, and E651D (Fig. 8). Both D154N and D562E were modeled to be in cytoplasmic linkers 1 and 4, respectively, yet they produced opposite shifts in apparent Na_i^+ affinity. D154N, like other acidic residues discussed thus far, displayed a slightly increased Na_i^+ affinity (K_m 43 ± 2 mM, Hill coefficient 3.0 ± 0.4, $n = 3$), but D562E displayed a substantially decreased affinity for Na_i^+ affinity (K_m = 107 ± 20 mM, Hill coefficient = 2.2 ± 0.4, $n = 3$). E651D on the other hand is modeled to be in the extracellular C terminus; this mutation resulted in one of the most profound decreases in Na_i^+ affinity that we observed in this study. We found that the derived normalized rates for E651D did not appear to reach saturation at the highest $[Na^+]_i$ tested, so as was described for I550A (Fig. 4),

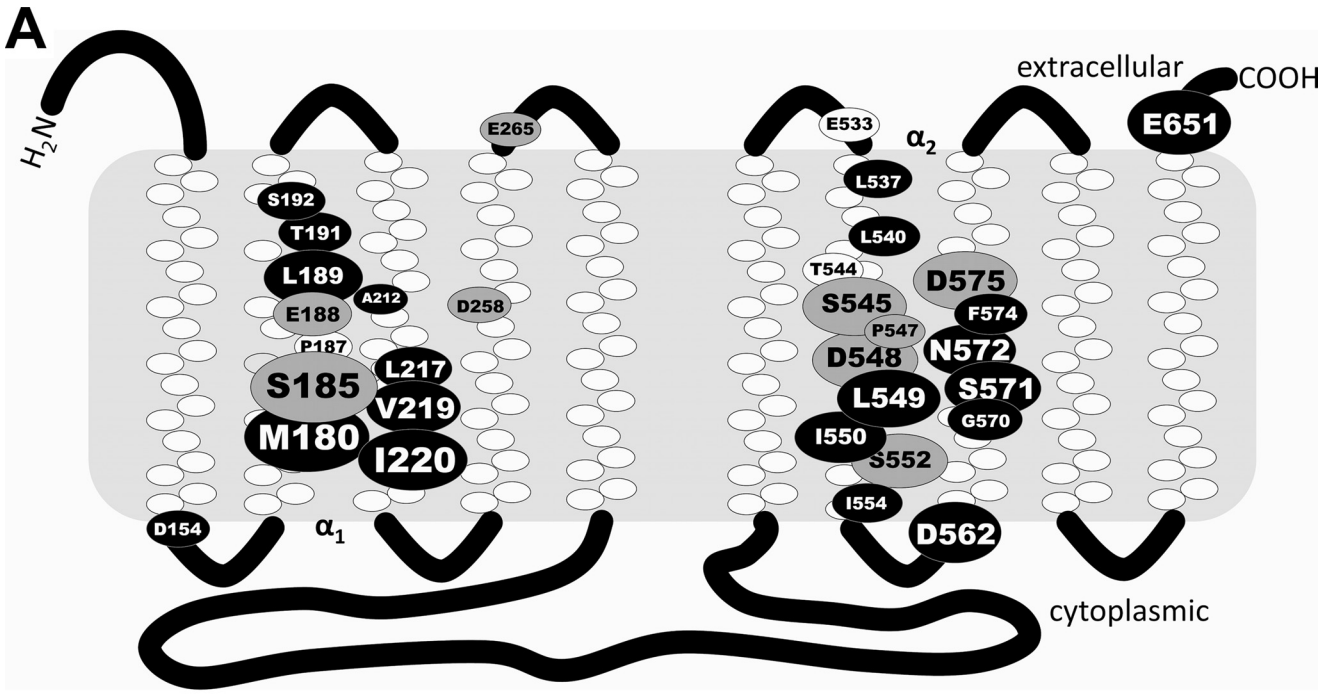

FIGURE 8. **Schematic representation of current topological model of NCKX2, and sequence alignment with NCX1.** *A*, our current topological model consists of two sets of transmembrane segments separated by a large intracellular loop. The positions of the α_1 and α_2 repeats are indicated, along with the modeled position of the residues studied in detail herein and in Refs. 24 and 25. The size of the *oval* represents the importance of the residue in Na^+ transport as judged by the magnitude of shift in apparent Na_i^+ affinity when substituted. *Black ovals* with *white lettering* are residues investigated herein whose substitution resulted in a shift in Na_i^+ affinity, *white ovals* with *black lettering* indicate residues whose substitution was previously shown to alter Ca^{2+} and K^+ affinity (24, 25), and *gray ovals* with *black lettering* indicate residues whose substitution we have found to alter both Na^+ and Ca^{2+}/K^+ affinity. *B*, amino acid sequence alignment of human NCKX2 (NP_065077.1) and canine NCX1 (P23685–1; isoform most widely used in structure-function studies) in the α_1 (*top sequence*) and α_2 (*bottom sequence*) repeat regions. Residues in NCX1 previously shown to produce shifts in Na^+ affinity when substituted for which the equivalent position residue in NCKX2 was analyzed in this study are highlighted by *bold type* (40). The details of the alignment are as in the legend to Fig. 1.

we normalized the rates for E651D to the average of the normalized rates measured with 175 and 200 mM $[Na^+]_i$, then compared the normalized rates at 75–100 mM $[Na^+]_i$, and found the values for E651D were substantially smaller than those of wt NCKX2 for the same range of $[Na^+]_i$ (Fig. 7). Substitution mutants of Arg^{557} and Lys^{558}, modeled to be in the cytoplasmic linker 4, were also tested but were found to not affect the apparent Na_i^+ of NCKX2 (Fig. 6); this is perhaps not surprising, because NCKX are cation exchangers, and coordination of cations does not require residues with positive side chain groups (34).

Ser and Thr Residues—Of the strictly conserved Ser and Thr residues in NCKX1–5, several were particularly interesting to us because they bracket the central acidic residues Glu^{188} and Asp^{548}. In this study, we tested S185A, T191A, S192A, T544S, S545A, S552T, S566A, and S571A. Three of these substitutions resulted in substantially decreased Na_i^+ affinity: S185A (Fig. 3), S545A, and S552T; these substitutions were analyzed using the averages of normalized rates at 75 and 100 mM $[Na^+]_i$ (Fig. 7). Two of our measurements of T544S also indicated a trend toward a large shift to decreased Na_i^+ affinity, but the compiled data were too scattered for that substitution mutant to draw a conclusion. T191A and S192A on the other hand, resulted in small but significant increases in Na_i^+ affinity (Fig. 6). We also chose to investigate substitutions of the $^{570}GSN^{572}$ stretch in transmembrane segment 9; this stretch is highly conserved among members of both NCKX1–5 as well as between NCKX and NCX (Figs. 1 and 8). We previously reported that N572C resulted in a substantial increase in Na_i^+ affinity (K_m for Na_i^+ = 16 ± 1 mM, Hill coefficient = 5.2 ± 1.8, n = 3), and likewise here we found that S571A displayed a comparable shift (K_m = 22 ± 2 mM, Hill coefficient = 3.9 ± 1.3, n = 3; Figs. 4*C* and 6),

whereas G570A displayed a slight trend toward an increased Na_i^+ affinity (K_m = 48 ± 3 mM, Hill coefficient = 3.3 ± 0.6, n = 3; Fig. 6).

Aliphatic Residues—C-terminal to both central acidic residues Glu^{188} and Asp^{548} are strictly conserved Leu residues; substitution of either Leu^{189} or Leu^{549} with Ala resulted in substantially decreased Na_i^+ affinity (K_m for L189A = 79 ± 3 mM, Hill coefficient = 2.3 ± 0.2, n = 3; K_m for L549A = 90 ± 15 mM, Hill coefficient = 2.8 ± 0.9, n = 3; Fig. 6). We also tested two substitutions at position Ile^{550}; although substitution with Ala resulted in greatly decreased Na_i^+ affinity (Figs. 4*D* and 7), substitution with Cys did not affect Na_i^+ affinity (K_m = 62 ± 4 mM, Hill coefficient = 2.5 ± 0.4, n = 3; Fig. 6), and functional activity of I550C was not greatly diminished (the V_{max} of I550A was 6% of wt NCKX2, whereas that of I550C was 41% of wt NCKX2). It is of interest to note that Ile^{550} is not strictly conserved among NCKX1–5, where the equivalent position in NCKX3–5 is Cys (Fig. 1). Additionally, we investigated several residue substitutions in the α_1 TM3, where a stretch of 14 amino acids is highly conserved between members of the NCKX and NCX families. Substitution mutant A212S resulted in a slightly increased Na_i^+ affinity (K_m = 42 ± 3 mM, Hill coefficient = 2.8 ± 0.6, n = 3; Fig. 6). Also within this stretch, we found that substitution of Leu^{217} with Ala increased Na_i^+ affinity substantially (K_m = 25 ± 2 mM, Hill coefficient = 2.1 ± 0.4, n = 3; Fig. 6). On the other hand, substitutions of either Val^{219} or Ile^{220} with Ala resulted in markedly decreased Na_i^+ affinity (K_m for V219A = 94 ± 14 mM, Hill coefficient = 2.8 ± 0.8, n = 3; K_m for I220A = 102 ± 15 mM, Hill coefficient = 2.3 ± 0.4, n = 3; Fig. 6).

DISCUSSION

NCKX, along with the K^+-independent NCX, are characterized by the capacity to transport multiple Na^+ ions/transport cycle and are unique in their absolute selectivity for Na^+ over any other alkali cation (28–30). This study was the first to examine a large number of conserved residues in a member of the *SLC24* gene family, NCKX2, to define the residues important in governing the transport of Na^+. We examined in total 102 single-residue substitutions; of the 39 selected for detailed analysis in this study, 31 were found to significantly impact Na_i^+ affinity by shifting the apparent affinity to either lower or higher values compared with the apparent K_m for wild type NCKX2 (58 mM Na^+). The method used to derive a measure of Na_i^+ affinity was based on monitoring increases in intracellular Ca^{2+} in HEK293 cells mediated by the Ca^{2+} entry mode of NCKX2 in response to Na^+ addition in the presence of gramicidin using the Ca^{2+} probes fluo-4FF and/or fluo-4. This method, used to monitor fluorescence from ensembles of transiently transfected HEK293 cells, allowed us to resolve the kinetic parameters of activity of mutants of NCKX2 that had activity as low as 1% that of wild type. Importantly, we did not observe a correlation between the level of activity (V_{max}) of a given single-residue substitution and altered Na_i^+ affinity (supplemental Table S1). A good example is the substitution G176A, which reduced V_{max} to 2% of wild type NCKX2; our interpretation is that Gly^{176} is an important residue for allowing conformational changes in the protein associated with its transport cycles. Nevertheless, the apparent Na_i^+ affinity of G176A was not altered with respect to that of wild type (Fig. 6). Moreover, we did not observe a correlation between the maximal transport activity observed for single-residue substitutions and the direction of the shift in apparent Na_i^+ affinity. We found residue substitutions resulting in moderate decreases in V_{max}, *e.g.* D548E (43% of wild type) and V219A (51% of wild type), that appeared to have shifts in Na_i^+ affinity of opposite direction: increased for D548E but decreased for V219A (Fig. 6). On the other hand, we found residue substitutions with greatly decreased V_{max}, *e.g.* S185A (7% of wild type) and L540A (5% of wild type), whose direction of shift in Na_i^+ affinity was also opposite in direction: decreased for S185A but increased for L540A (Figs. 6 and 7).

For all of the NCKX2 mutants that showed an increase in Na_i^+ affinity, the normalized rate values increased steeply in the range of $[Na^+]_i$ = 10–75 mM and declined for the higher $[Na^+]_i$ values tested (*e.g.* Figs. 4 and 5 and supplemental Fig. S3). This strongly suggests that an increase in Na_i^+ affinity is accompanied by an increase in Na_o^+ affinity, which leads to increased competition between external Na^+ and Ca^{2+}. This observation is consistent with the alternating access model of NCKX transport, in which a single set of residues is responsible for cation binding in both inward and outward facing conformations.

As expected for a membrane cation transporter (34), most of the residues we found to substantially alter Na^+ affinity in NCKX2 are oxygen-bearing polar side chain residues (Ser^{185}, Ser^{545}, Ser^{552}, Ser^{571}, and Asn^{572}) or negatively charged side chain residues (Asp^{548}, Asp^{562}, Asp^{575}, and Glu^{651}). Of the residues identified herein, our results reinforce the central importance of the mid-membrane plane acidic residues Glu^{188}, Asp^{548}, and Asp^{575} in coordinating cation substrates, because mutation of any of these has now been shown to alter the apparent affinity for both Ca^{2+} and K^+ (24, 25), in addition to affinity for counter-transported Na^+ in our current work. Additionally, the Ser/Thr residues that bracket the centrally located Glu^{188} and Asp^{548} by one helical turn, previously shown to be important for Ca^{2+} + K^+ transport (24, 35), have now also been shown to be important for Na^+ transport as well. This lends support to our proposal that residues Ser^{185}, Glu^{188}, and Thr^{191}/Ser^{192} in TM2; Thr^{544}/Ser^{545}, Asp^{548}, and Ser^{552} in TM8; and Ser^{571}/Asn^{572}, and Asp^{575} in TM9 (Fig. 8), likely line the hydrophilic surface extending from the binding pocket in the mid-membrane plane defined by Glu^{188} and Asp^{548} to the ion access port at the membrane/aqueous environment interface. Using site-directed disulfide mapping, we have previously shown that many of those residues are in close proximity to one another (22). Another novel feature of our current findings to note is that many residue substitutions were found to specifically impact Na^+ affinity and that those residues span most of the length of the predicted TM domains (from Ile^{220} to Leu^{537}; Fig. 8), perhaps reflecting the fact that multiple (four) Na^+ ions must be simultaneously accommodated by NCKX2. Additional negatively charged residues thought to be located at the membrane interface were found to alter apparent Na^+ affinity when substituted: D154N, D562E, and E651D. D562E and E651D in particular were among the largest shifts we observed in the ~30 residue substitutions found to alter Na^+ affinity in this study; both decreased apparent Na_i^+ affinity. Such residues may form part of a selectivity filter at the aqueous vestibule leading to the

cation binding pocket in the mid-membrane plane, analogous to selectivity filters of voltage-gated cation channels (36, 37).

Other than negatively charged or polar side chain residues, we also found a large number of aliphatic residues (Leu^{189}, Leu^{217}, Val^{219}, Ile^{220}, Leu^{537}, Leu^{540}, Leu^{549}, and Ile^{550}) to considerably affect Na^+ affinity when substituted; possibly also the two proline residues (Pro^{187} and Pro^{547}). Such residues may affect the helical propensity of the transmembrane segments bearing these residues and, therewith, cause subtle alterations in the positioning of other residues directly involved in Na^+ binding. For example, the *GXXXP* motif found in both TM2 and TM8 may cause local unwinding of the α-helix into a helix-loop-helix motif that is often found in structures of secondary transporters (16, 17, 20, 21). This would also make available main chain carbonyl oxygens of aliphatic residues for cation liganding, as has been shown in crystal structures of the Na^+-coupled galactose transporter and Leu transporter (16, 20). Additionally, two residues whose side chains do not contain oxygens, Met^{180} and Phe^{574}, were also found among the residues that greatly decreased apparent Na_i^+ affinity (Fig. 7); such residues may be gating residues that partially or transiently occlude liganded Na^+ ions from extra- or intracellular hydrophilic vestibules; Met and Phe have been observed to occlude access to the hydrophilic vestibule to one side of the membrane in the Na^+-coupled galactose transporter (16).

Of particular interest to note, previous functional analysis of mammalian Na^+/K^+ ATPase and Na^+/Ca^{2+} exchanger (NCX, gene family *SLC8*), two other plasma membrane transporters that transport multiple Na^+ ions (three each in the case of those proteins), have found that substitution of aliphatic residues can impact on Na^+ affinity. Examples of specific aliphatic or otherwise uncharged side chain residues in Na^+/K^+ ATPase that have been found to be of importance to Na^+ liganding and/or transport are Val^{920} (38), Leu^{91}, and Phe^{95} (39). NCKX and NCX on the other hand, although functionally regarded as closely related proteins, in fact share only limited structural similarity in terms of amino acid sequence, essentially restricted to the α_1 and α_2 repeats (Fig. 8). It is noteworthy that 16 of 25 residues in the α_1 and α_2 repeats that we report here to affect Na_i^+ affinity are conserved between NCX1 and NCKX2 with many of the remainder being conservative substitutions, *e.g.* Val to Ile or Leu (Fig. 8). In the α_1 repeat, the region of ^{210}GSAVFNILFVI^{220} in TM3, which is highly conserved between NCKX paralogs as well as between NCKX and NCX (Figs. 1 and 8), was found in our current study to be a region that is particularly sensitive to mutagenesis when assayed for Na^+ affinity. It harbors three residues, Gly^{210}, Ser^{211}, and Asn^{215} (which we believe to be a critical residue for ion coordination), for which no substitution tested provided sufficient functional activity for assessment of Na^+ affinity (<1% of wild type NCKX2 activity; protein expression as judged by Western blot was normal; see supplemental Fig. S2). In NCX, several residues were investigated in TM3, and the following were found to have strong effects on Na^+ affinity when substituted: Ala^{140}, Phe^{145}, and Ile^{147} (40). The equivalent position residues in NCKX were among the residues selected for further analysis for Na^+ affinity in this study: A212S (equivalent to Ala^{140} in NCX1), L217A (equivalent to Phe^{145}), and V219A (equivalent to Ile^{147}). We found that substitution of the equivalent position residues in NCKX also resulted in shifts in Na_i^+ affinity; the shift was subtle in the case of A212S but strong in the case of L217A and V219A. We also studied I220A, which is conserved in NCX1 and also produced a strongly decreased Na_i^+ affinity (Fig. 6). If these residues do participate directly in ion coordination, TM3 would need to be unwound locally to expose main chain carbonyl groups. However, there are no obvious helix breakers (Pro or Gly) in TM3; future studies will aim to investigate the structural nature of TM3 as well as other TMs in NCKX2.

A major prediction of the alternating access model of membrane transport is that the same binding pocket/set of residues would be expected to bind ligand on one side of the membrane and counter-transported cargo on the trans-side of the membrane. We found in this study that most NCKX2 residues previously found to have a substantial effect on Ca^{2+} and K^+ when substituted (shifts in Ca^{2+} and K^+ were always comparable for the same residue substitution) also do impact on the apparent Na^+ affinity, including the acidic residues Glu^{188} and Asp^{548}, the serines Ser^{185} and Ser^{545}, and the K^+ affinity defining residue Asp^{575}, which we found to also impact on Na^+ affinity (Figs. 6 and 8). Fig. 8 also illustrates that many residues shown here to influence Na^+ affinity have not yet been investigated for changes in Ca^{2+} and K^+ affinity. A comprehensive survey of residues important for Ca^{2+} and K^+ affinities similar to that carried here for Na^+ is currently underway. These results, taken together with the observation that Na^+ can compete with either Ca^{2+} or K^+ for the exchanger binding pocket, lend support to the alternating access or consecutive access functional model for the operation of NCKX and other ion transporters.

REFERENCES

1. Schnetkamp, P. P., Basu, D. K., and Szerencsei, R. T. (1989) *Am. J. Physiol.* **257,** C153–C157
2. Schnetkamp, P. P., Szerencsei, R. T., and Basu, D. K. (1991) *J. Biol. Chem.* **266,** 198–206
3. Cervetto, L., Lagnado, L., Perry, R. J., Robinson, D. W., and McNaughton, P. A. (1989) *Nature* **337,** 740–743
4. Prinsen, C. F., Szerencsei, R. T., and Schnetkamp, P. P. (2000) *J. Neurosci.* **20,** 1424–1434
5. Paillart, C., Winkfein, R. J., Schnetkamp, P. P., and Korenbrot, J. I. (2007) *J. Gen. Physiol.* **129,** 1–16
6. Tsoi, M., Rhee, K. H., Bungard, D., Li, X. F., Lee, S. L., Auer, R. N., and Lytton, J. (1998) *J. Biol. Chem.* **273,** 4155–4162
7. Li, X. F., Kiedrowski, L., Tremblay, F., Fernandez, F. R., Perizzolo, M., Winkfein, R. J., Turner, R. W., Bains, J. S., Rancourt, D. E., and Lytton, J. (2006) *J. Biol. Chem.* **281,** 6273–6282
8. Cuomo, O., Gala, R., Pignataro, G., Boscia, F., Secondo, A., Scorziello, A., Pannaccione, A., Viggiano, D., Adornetto, A., Molinaro, P., Li, X. F., Lytton, J., Di Renzo, G., and Annunziato, L. (2008) *J. Neurosci.* **28,** 2053–2063
9. Dong, H., Jiang, Y., Triggle, C. R., Li, X., and Lytton, J. (2006) *Am. J. Physiol. Heart Circ. Physiol.* **291,** H1226–H1235
10. Kraev, A., Quednau, B. D., Leach, S., Li, X. F., Dong, H., Winkfein, R., Perizzolo, M., Cai, X., Yang, R., Philipson, K. D., and Lytton, J. (2001) *J. Biol. Chem.* **276,** 23161–23172
11. Li, X. F., Kraev, A. S., and Lytton, J. (2002) *J. Biol. Chem.* **277,** 48410–48417
12. Ginger, R. S., Askew, S. E., Ogborne, R. M., Wilson, S., Ferdinando, D., Dadd, T., Smith, A. M., Kazi, S., Szerencsei, R. T., Winkfein, R. J., Schnetkamp, P. P., and Green, M. R. (2008) *J. Biol. Chem.* **283,** 5486–5495
13. Lamason, R. L., Mohideen, M. A., Mest, J. R., Wong, A. C., Norton, H. L., Aros, M. C., Jurynec, M. J., Mao, X., Humphreville, V. R., Humbert, J. E., Sinha, S., Moore, J. L., Jagadeeswaran, P., Zhao, W., Ning, G., Makalowska,

I., McKeigue, P. M., O'donnell, D., Kittles, R., Parra, E. J., Mangini, N. J., Grunwald, D. J., Shriver, M. D., Canfield, V. A., and Cheng, K. C. (2005) *Science* **310,** 1782–1786
14. Vogel, P., Read, R. W., Vance, R. B., Platt, K. A., Troughton, K., and Rice, D. S. (2008) *Vet. Pathol.* **45,** 264–279
15. Kinjo, T. G., Szerencsei, R. T., Winkfein, R. J., Kang, K., and Schnetkamp, P. P. (2003) *Biochemistry* **42,** 2485–2491
16. Faham, S., Watanabe, A., Besserer, G. M., Cascio, D., Specht, A., Hirayama, B. A., Wright, E. M., and Abramson, J. (2008) *Science* **321,** 810–814
17. Hunte, C., Screpanti, E., Venturi, M., Rimon, A., Padan, E., and Michel, H. (2005) *Nature* **435,** 1197–1202
18. Iwamoto, T., Uehara, A., Imanaga, I., and Shigekawa, M. (2000) *J. Biol. Chem.* **275,** 38571–38580
19. Nicoll, D. A., Ottolia, M., Lu, L., Lu, Y., and Philipson, K. D. (1999) *J. Biol. Chem.* **274,** 910–917
20. Yamashita, A., Singh, S. K., Kawate, T., Jin, Y., and Gouaux, E. (2005) *Nature* **437,** 215–223
21. Yernool, D., Boudker, O., Jin, Y., and Gouaux, E. (2004) *Nature* **431,** 811–818
22. Kinjo, T. G., Kang, K., Szerencsei, R. T., Winkfein, R. J., and Schnetkamp, P. P. (2005) *Biochemistry* **44,** 7787–7795
23. Winkfein, R. J., Szerencsei, R. T., Kinjo, T. G., Kang, K., Perizzolo, M., Eisner, L., and Schnetkamp, P. P. (2003) *Biochemistry* **42,** 543–552
24. Kang, K. J., Kinjo, T. G., Szerencsei, R. T., and Schnetkamp, P. P. (2005) *J. Biol. Chem.* **280,** 6823–6833
25. Kang, K. J., Shibukawa, Y., Szerencsei, R. T., and Schnetkamp, P. P. (2005) *J. Biol. Chem.* **280,** 6834–6839
26. Jardetzky, O. (1966) *Nature* **211,** 969–970
27. Mitchell, P. (1957) *Nature* **180,** 134–136
28. DiPolo, R., and Beaugé, L. (2006) *Physiol. Rev.* **86,** 155–203
29. Doering, A. E., Nicoll, D. A., Lu, Y., Lu, L., Weiss, J. N., and Philipson, K. D. (1998) *J. Biol. Chem.* **273,** 778–783
30. Schnetkamp, P. P. (1986) *J. Physiol.* **373,** 25–45
31. Altimimi, H. F., and Schnetkamp, P. P. (2007) *J. Biol. Chem.* **282,** 3720–3729
32. Motulsky, H., and Christopoulos, A. (2004) *Fitting Models to Biological Data Using Linear and Nonlinear Regression: A Practical Guide to Curve Fitting,* pp. 134–186, Oxford University Press, Oxford
33. Sharon, D., Yamamoto, H., McGee, T. L., Rabe, V., Szerencsei, R. T., Winkfein, R. J., Prinsen, C. F., Barnes, C. S., Andreasson, S., Fishman, G. A., Schnetkamp, P. P., Berson, E. L., and Dryja, T. P. (2002) *Invest. Ophthalmol. Vis. Sci.* **43,** 1971–1979
34. Gouaux, E., and Mackinnon, R. (2005) *Science* **310,** 1461–1465
35. Visser, F., Valsecchi, V., Annunziato, L., and Lytton, J. (2007) *J. Biol. Chem.* **282,** 4453–4462
36. Heginbotham, L., Lu, Z., Abramson, T., and MacKinnon, R. (1994) *Biophys. J.* **66,** 1061–1067
37. Heinemann, S. H., Terlau, H., Stühmer, W., Imoto, K., and Numa, S. (1992) *Nature* **356,** 441–443
38. Imagawa, T., Yamamoto, T., Kaya, S., Sakaguchi, K., and Taniguchi, K. (2005) *J. Biol. Chem.* **280,** 18736–18744
39. Einholm, A. P., Andersen, J. P., and Vilsen, B. (2007) *J. Biol. Chem.* **282,** 23854–23866
40. Ottolia, M., Nicoll, D. A., and Philipson, K. D. (2005) *J. Biol. Chem.* **280,** 1061–1069
41. Larkin, M. A., Blackshields, G., Brown, N. P., Chenna, R., McGettigan, P. A., McWilliam, H., Valentin, F., Wallace, I. M., Wilm, A., Lopez, R., Thompson, J. D., Gibson, T. J., and Higgins, D. G. (2007) *Bioinformatics* **23,** 2947–2948